Journal of Power Sources 244 (2013) 196–206

Contents lists available at SciVerse ScienceDirect

Journal of Power Sources

journal homepage: www.elsevier.com/locate/jpowsour

# Technological potential and issues of polyacrylonitrile based nanofiber non-woven separator for Li-ion rechargeable batteries

Yeon-Joo Kim [a], Hyun-Soo Kim [a], Chil-Hoon Doh [a], Seok Hong Kim [b], Sang-Min Lee [a,*]

[a] Battery Research Center, Korea Electrotechnology Research Institute, Changwon 641-120, Republic of Korea
[b] R&D Center, Finetex EnE, 350, Bukyang-dong, Hwasung-si, Gyeonggi-do, Republic of Korea

## HIGHLIGHTS

- PAN separator has higher ionic conductivity and lower thermal shrinkage.
- Battery employing PAN separator shows superior performance over PE separator's one.
- PAN separator couldn't prevent metal complex from being deposited on anode surface.

## ARTICLE INFO

*Article history:*
Received 11 October 2012
Received in revised form
25 January 2013
Accepted 29 January 2013
Available online 6 February 2013

*Keywords:*
Lithium-ion battery
Micro-porous membrane separator
Non-woven separator
Ion tranport

## ABSTRACT

We investigate on the technological potential and issues of non-woven separator as an alternative to conventional separator in terms of various evaluation points. Thus, optimal evaluation systems for new nonwoven polyacrylonitrile (PAN) separator are proposed to compare with commercialized polyethylene (PE) separator, and corresponding stacking-type pouch batteries are used as an evaluation tool. Cell performance, electrochemical stability, and thermal stability for both separators are compared. Based on the comparison results, each separator's effects are discussed in detail. In comparison to PE separator, the non-woven separator exhibits distinct advantage in microporous structure, leading to superior reliability of cell. Based on the understanding of non-woven separator, cell performances of the separator at different charge/discharge conditions are discussed in terms of ion transport of the separator and AC impedance of the cell. Moreover, the problems of nonwoven separator to be solved are clearly stated through the phenomenological analyses. The overall evaluation results indicate that the non-woven PAN separator has many advantages over the PE separator, which, in turn, contribute to superior cell performances. Therefore, the PAN nonwoven membrane can be the most promising candidate for separators of the next generation of lithium-ion battery if the problems to be stated will be solved.



## 1. Introduction

Lithium-ion batteries are widely used for electronic devices such as mobile phones, laptop computers, and digital cameras due to their high energy density and long life cycle. With the search for a solution as alternative propulsion system, lithium-ion batteries are also expected to be an alternative power source for Plug-in Hybrid Electric Vehicle (PHEV), particularly with increasing needs for alternative energy and environment protection, due to the advantages in longer cycle life, higher voltages and energy density when compared with other rechargeable batteries [1–6].

As lithium-ion batteries used in the electric car sector require high-capacity and high-power performance, certain safety features (i.e. ignition, explosion, etc.) become more critical. Lithium, a highly-reactive anode material, may cause an explosion if it comes into direct contact with the cathode [7–13]. Therefore, an electrically insulating membrane to separate the anode from the cathode is critical component for the safety of a battery. Most membranes used for lithium-ion batteries are polyolefin types. However, thermal contraction coupled with physical damage occurs when polyolefin is exposed to high temperatures over 100 °C due to its physical properties and manufacturing process, which could result in a possible short-circuiting inside a battery. There have been numerous studies to overcome these problems related to current polyolefin separators [14,15].

A micro-porous membrane is necessary for separating positive and negative electrodes and for maintaining liquid electrolyte between

* Corresponding author. Tel.: +82 55 280 1663; fax: +82 55 280 1590.
*E-mail addresses:* sangma@keri.re.kr, sangminlee71@gmail.com (S.-M. Lee).

0378-7753/$ – see front matter © 2013 Elsevier B.V. All rights reserved.
http://dx.doi.org/10.1016/j.jpowsour.2013.01.166

both electrodes. However, the existence of a separator increases the cell resistance by a factor and reduces the volumetric energy density of the battery. Polyolefin micro-porous membranes have been used as major separators for lithium ion batteries. But, the rate capabilities of the separators are not enough for high-power applications, such as electric vehicles, hybrid electric vehicles and robots. The micro-porous membrane separators have some disadvantages that need to be improved, such as low wettability, low porosity of about 40% [16], and thermal shrinkage that causes short circuits between electrodes under unusual heat generation. Recently, various approaches to overcome these shortcomings of polyolefin based separators have been reported. Most reports focused on many alternatives of polyolefin based separators such as non-woven separators and inorganic composite [17–21,24]. In contrast, non-woven separators have higher porosity (60–90%) and higher air permeability [22] than polyolefin, which could be used to increase the rate capability of lithium ion batteries. In addition, excellent thermal tolerance at high temperature up to 180 °C can be expected, thanks to low thermal-shrinkage.

Some notable studies focusing on non-woven, ceramic composite, co-extrusion & electrolyte affinity technologies have been very active. Also, there have been some findings on the application of a PAN separator to a rechargeable lithium battery, utilizing aramid-based non-wovens and PAN-based nano-fibers. Cho et al. [23] has reported on the electrochemical performance of PAN nanofiber based non-woven separator for lithium ion batteries. They showed the superior performances of non-woven separator based battery in view of its reliability such as rate capability and cycle life, etc. Furthermore, the thermal stability of battery was reported to be remarkably improved by applying PAN based non-woven based separator [18]. There still, however, remain some process issues to be solved due to the inferiority in its physical properties such as low tensile strength, and puncture strength [24]. In spite of this physical drawback, the PAN based non-woven separator has been regarded as effective for thermal battery safety and low cost, as the demand for large-capacity batteries for electric cars has significantly increased. Most importantly, the PAN based non-woven separator was not overall seen if it will be feasible component in many different aspects of battery.

In this study, an optimal evaluation system for current PE separator and new PAN separator was come up with, and corresponding stacking-type pouch batteries were designed. Batteries with PE separators were electrically, thermally, electrochemically and chemically compared to those with PAN separators. Based on the comparison results, each separator's effects were extensively investigated and analyzed.

## 2. Experiments

### 2.1. Fabrication of the PAN-based non-woven separator

The non-woven separator was fabricated by electro-spinning process. The electro-spinning solution was prepared by dissolving polyacrylonitrile (PAN, Mw = 150,000, Aldrich) powder in N, N-dimethylformamide (DMF, Aldrich) at room temperature. The prepared solution was put into 10 ml syringes with metal needles. A power supply (SHV200/Conver Tech) was used to provide the potential difference (1.9 V) for electro-spinning process. Needle-to-collector distance was set as 18 cm and electro-spun fibers were collected on an aluminum foil. After that, the electrospun fibers were hot-pressed to be non-woven separator of 25 μm thickness at 70 °C.

### 2.2. Design of PAN-separator-based rechargeable lithium batteries

PAN separators provided by Finetex EnE, Inc. were stacked by the stack-fold method to make full-pouch cells with the design capacity of 300 mAh. Before making the full cell, the design specifications for the anode/cathode/electrolyte were taken into consideration. Enhanced natural graphite materials (mostly IT & high-output uses) were used as active materials for an anode. The core anode material is natural graphite with core–shell type, while the surface of natural graphite is coated with amorphous carbon layer. In addition, SBR/CMC water-based binders were added to attain a loading level (20 $mgcm^{-2}$) per unit area and electrode density of 1.51 $gcc^{-1}$. Typical high-output active materials such as $Li(Ni_{1/3}Co_{1/3}Mn_{1/3})O_2$ (LNCMO) were used for the cathode, while super-P and PVDF binder were used as a conducting agent and a binder, respectively. The cathode was designed to attain a corresponding loading level (39 $mgcm^{-2}$) and electrode density (3.64 $gcc^{-1}$). The electrolyte specifications were set at 1 M $LiPF_6$, EC/EMC = 1:2(v/v) + VC 2 wt. %. Furthermore, PE separators (provided by Celgard Co. Ltd.) with similar thickness (~26 μm) were compared to PAN separators in order to evaluate each separator type's performance. In order to establish a full-cell evaluation, the design specifications for a corresponding battery were set at an $n/p$ ratio of 1.1 and a current density of 2.5 $mAcm^{-2}$. In addition, there was a 2 mm variation in the widths of the anode, cathode and separator, in order to prevent any short-circuiting between the anode and cathode.

### 2.3. Analysis of PAN-separator-based rechargeable lithium batteries

FE-SEM (Hitachi Co. S-4800) was used to observe the structures of PAN separator and PE separator, and each separator's electrochemical reliability, electrochemical stability and thermal stability were accordingly evaluated.

#### 2.3.1. Electrochemical reliability

For evaluation of electrochemical reliability, the related charge/discharge performances were measured in a voltage range between 3.0 V and 4.2 V (by CC (constant current)–CV (constant voltage)) on charge/discharge curves. Rate capability was evaluated at current of 0.2 C charge and 0.1 C discharge. Also, the cyclic durability was measured at room temperature (25 °C) and high temperature (45 °C) while the C-rate was set at 1 C. For the analysis on electrochemical properties of each separator, low-temperature discharge properties and high-rate discharge capacity were evaluated and discussed with physical properties of separator. The low-temperature discharge properties and ion conductivity were tested with 0.2 C-charging & 0.5 C-discharging between 2.75 V and 4.2 V at −20, −10, 0, and 25 °C. At each temperature, the ion conductivity of each fully-charged separator was derived from AC impedance spectra. AC impedance was analyzed for the fully-charged cell using IM6 (ZAHNER, Germany). The frequency range was measured in 1 mHz–100 kHz, and amplitude was measured in 10 mV. The high-rate discharge capacity was also tested with 0.2 C-charging & 1 C/2 C/4 C/10 C-discharging between 2.75 V and 4.2 V.

#### 2.3.2. Electrochemical stability

For the evaluation of electrochemical stability during cell operation, the LSV (Linear Sweep Voltammetry) analysis was conducted on each separator. The measurement was performed in a two-electrode electrochemical system consisting of a SUS (stainless steel blocking electrode) working electrode, and lithium counter electrodes at room temperature. LSV was scanned between 3 V and 6 V at a rate of 20 mV $s^{-1}$. The full cell with each separator was fully charged up to 4.2 V under CC/CV trickling charging mode and then the surface of each separator was analyzed with SEM-EDS (Hitachi Co. S-4800).

#### 2.3.3. Thermal stability

For the evaluation of thermal stability, each separator was positioned between slide glasses and subjected to certain tensile

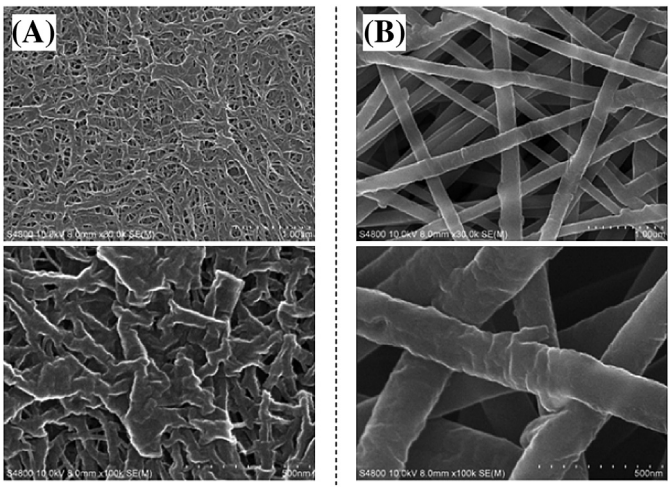


**Fig. 1.** SEM images of A) PE separator and B) PAN separator applied in pouch type full cell.

**Table 1**
Brief physical properties of separators.

| Property | PE separator | PAN separator |
|---|---|---|
| Thickness (μm) | 26 | 25 |
| Tensile strength (MPa) | 159 | 32 |
| Porosity (%) | 44 | 54 |
| Ionic conductivity ($mScm^{-1}$) | 0.63 | 0.76 |
| Electrolyte uptake (%) | ~116 | ~174 |

shear stress. Then, the temperature was raised to 150 °C and 180 °C at 5 °C per minute, and both separators were kept for 12 h at each temperature in order to compare their contraction percentages. In general, thermal abuse tolerance was studied using calorimetric techniques on full cell. In this work, ARC (Accelerated Rate Calorimetry) was used to see how the thermal contraction characteristics of separators affect the thermal tolerance of pouch full cell [25].

A maximum temperature of 450 °C was set to prevent uncontrolled thermal runaway and explosive decomposition of the cells in the ARC apparatus (TIAX Model). The ARC is operated in a "heat", "wait", "search" mode to detect the onset point of self-heating. The ARC increases the system's temperature in discrete steps ("heat"), waits for the thermal transients to decay ("wait") and then monitors the temperature of the cell for a fixed time period ("search"). If the cell temperature is not increasing above a threshold value, typically 0.02 °C $min^{-1}$, the temperature is increased by another step and the process repeated. If the cell temperature increases at rate equal or above the threshold value, the ARC switches to the exothermic mode during which the ARC temperature closely matches the cell temperature, thus maintaining the adiabatic state. The normal mode of operation of ARC terminates an experiment by cooling the sample once it reaches a set upper temperature limit or maximum temperature. The ARC experiment closely simulates

**Table 2**
1st and 2nd cycle data for pouch type full cell with (A) PE and (B) PAN separators.

| Cycle No | PE separator based cell | | | PAN separator based cell | | |
|---|---|---|---|---|---|---|
| | C-capacity (mAh) | D-capacity (mAh) | Efficiency (%) | C-capacity (mAh) | D-capacity (mAh) | Efficiency (%) |
| 1st | 372 | 318 | 85 | 375 | 320 | 85 |
| 2nd | 332 | 325 | 97 | 338 | 336 | 99 |

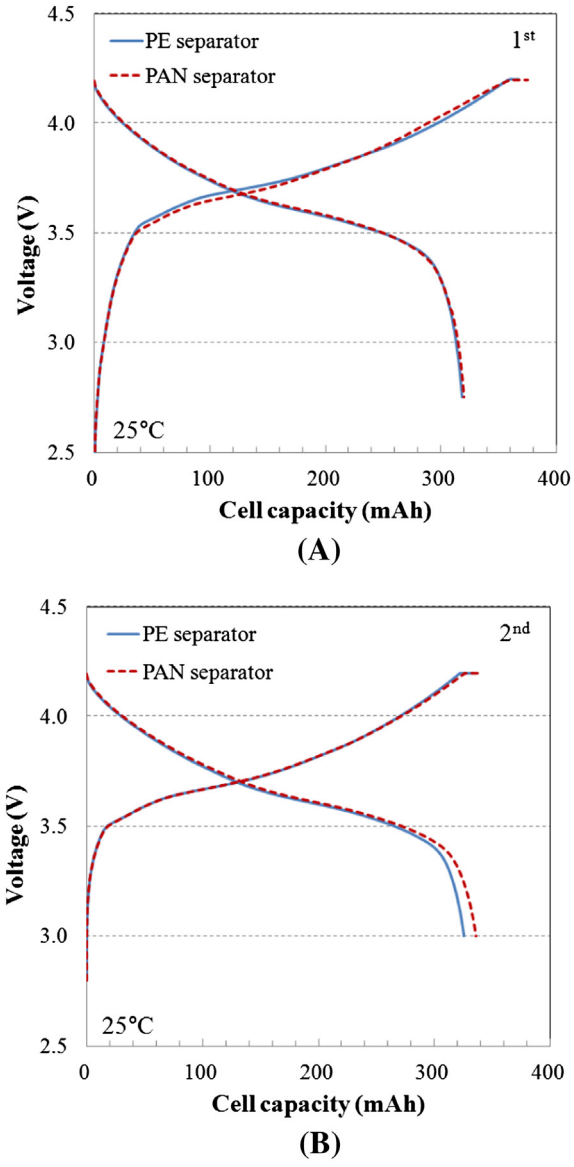


**Fig. 2.** Comparison of charge and discharge curves of pouch type full cell with PE and PAN separators at charge (0.2 C)–discharge (0.1 C) rate.

a thermal abuse environment that includes moderately high temperatures for relatively long periods of time. The details on ARC apparatus are described in Ref. [26]. In this experiment, the battery sample were heated between 50 and 400 °C at the rate of 5 °C $min^{-1}$ in the search for self-heating at the sensitivity threshold of 0.05 °C $min^{-1}$.

## 3. Results and discussion

### *3.1. Comparisons of physical properties between PE and PAN based separators*

The PE separator shows (Fig. 1(A)) a net structure with many open pores and these pores are uniformly distributed. On the other hand, as shown in Fig. 1(B), a number of nano-fibers can be observed by SEM analysis. The fibers exhibit homogeneous diameters and any observable beads do not exist on the fibers. In contrast to a PE separator having large number of small-sized micropores, of which average diameter appears to be below 0.1 μm,

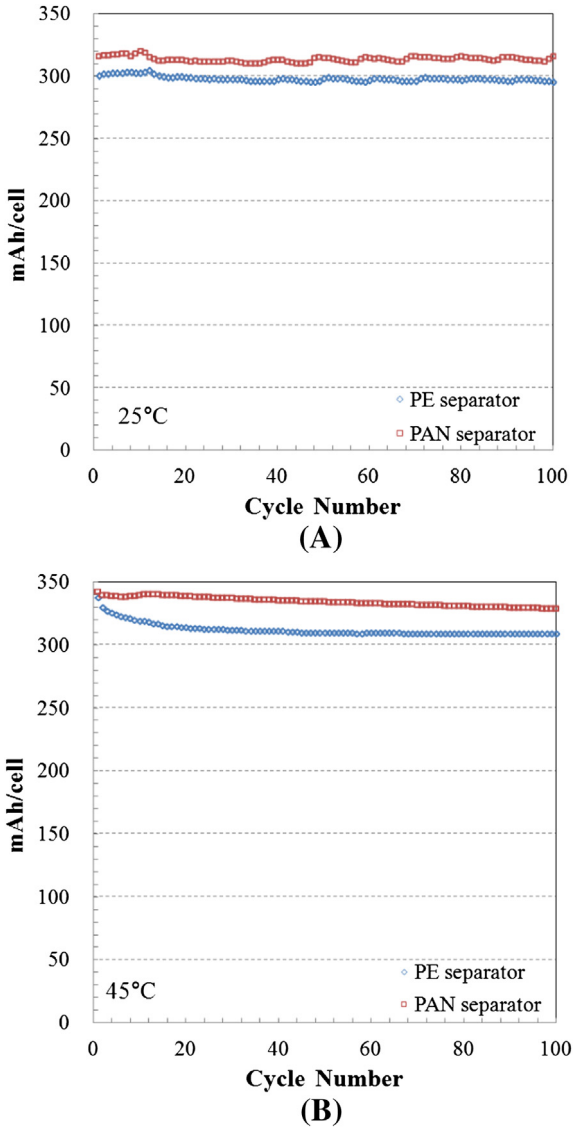


**Fig. 3.** Comparison of capacity retention of pouch type full cell with PE and PAN separators at (A) room temperature (25 °C) and (B) elevated temperature (45 °C).

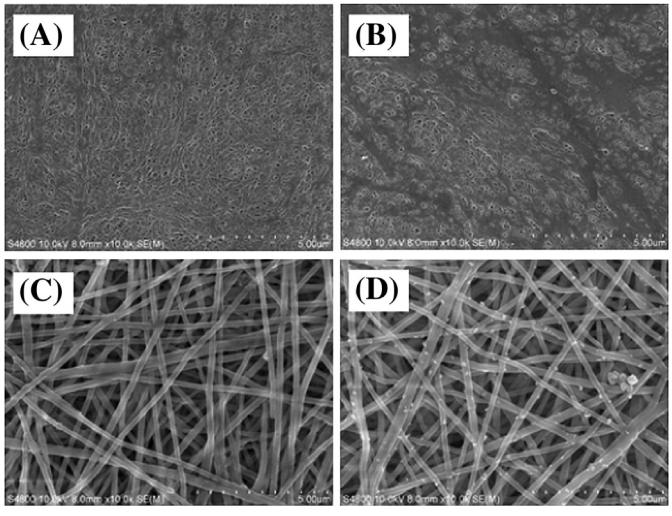


**Fig. 4.** Comparison of separator morphologies after 100th cycles at room temperature (A:PE, C:PAN) and elevated temperature (B:PE, D:PAN).

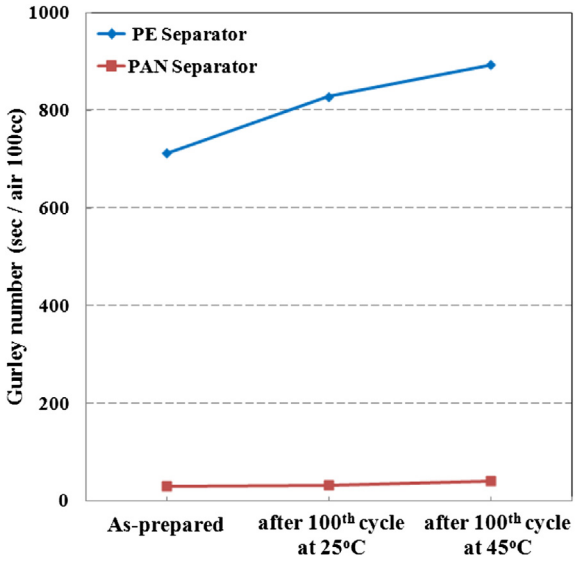


**Fig. 5.** Comparison of Gurley index after 100th cycles at room temperature and elevated temperature.

the pristine PAN non-woven shows excessively large-sized (0.3–0.5 μm) pores that are arbitrarily distributed between the PAN fibers. It is well known that various physical properties of separator are closely related with its morphologies. Table 1 shows brief physical properties of the PAN separator, compared with that of the conventional PE separator. The measured thickness of the PAN separator is in the range of 26 μm, of which values are similar to that of the PE separator. In spite of similar thickness, the PAN based non-woven separator has much lower tensile strength than conventional PE separator. In general, the non-woven separator doesn't have enough tensile strength to apply the current process of cell fabrication due to its morphological characteristics. Thus, the stack and folding process are employed to assemble the evaluation cell due to lack of tensile strength of PAN separator in this work. Indeed, the tensile strength of non-woven separator can be further improved by optimizing several key parameters such as fiber diameter and molecular weight, etc [27,28]. In particular, the PAN separator showed roughly 10% higher porosities than that of the PE separator. The ion conductivity of the PAN separator reaches $7.6 \times 10^{-1}$ S cm$^{-1}$ at 25 °C, which is higher than that of the PE separator ($6.3 \times 10^{-1}$ S cm$^{-1}$) at room temperature. Besides, the PAN separator is easily wetted by the liquid electrolyte and also affords larger electrolyte uptake (PAN separator ~174% vs. PE separator ~116%). These physical properties of separator were measured by referring description in previous reports [29].

### 3.2. Comparisons of unit cell performance between PE and PAN based separators

#### 3.2.1. Formation charge/discharge curves

The performances of batteries with the PE separator and PAN separator were investigated. At the first cycle, the cells were

**Table 3**
Gurley index of the PE separator and PAN separators after 100th cycle at 25 °C, and 45 °C.

| PE separator | Gurley (s) | PAN separator | Gurley (s) |
|---|---|---|---|
| As-prepared | 712.9 | As-prepared | 30.8 |
| After 100th cycle at 25 °C | 828.9 | After 100th cycle at 25 °C | 32.9 |
| After 100th cycle at 45 °C | 894.5 | After 100th cycle at 45 °C | 40.9 |

charged up to 4.2 V under constant current–constant voltage mode, and then discharged to 2.75 V under constant current mode. The initial charge–discharge cycles were tested with a 0.1 C-rate. The following formation cycle charge–discharge tests were charged up to 4.2 V (0.2 C) under constant current–constant voltage mode, and then discharged to 3 V (0.1 C) under constant current mode.

A cell's design capacity was set at 320 mAh. A pouch battery's 0.2 C standard capacity was measured to be 101–105% of the corresponding designed capacity (325 mAh ~ 336 mAh), and the battery became fully activated (reversible efficiency over 99%) in the second cycle. (Table 2) In addition, the charge/discharge behavior was observed to be almost similar between two-separators. Any unstable voltage profiles were not observed for the cells with the both separator as shown in Fig. 2. Both cells shows the similar discharge capacity at the 1st cycle but in case of PAN based cell, the reversible efficiency of more than 99% was attained earlier than that of PE's.

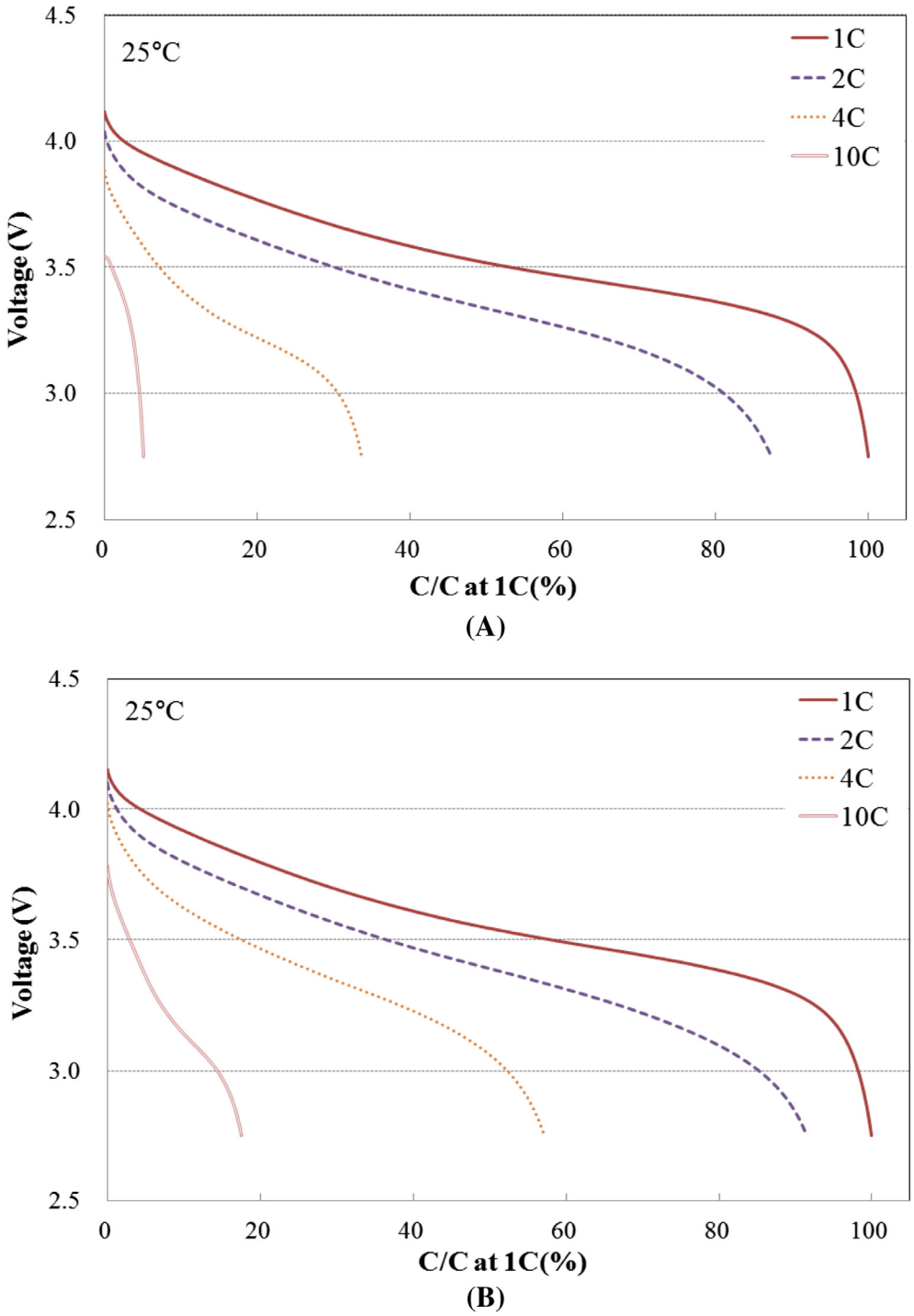


**Fig. 6.** Comparison of high-rate discharge properties of pouch type full cell with PE and PAN separators. (A) Change of discharge curves with C-rates (0.1, 1, 2, 4 and 10C) after CC–CV charging at 0.2 C to 4.2 V at room temperature for PE based pouch type full cell. (B) Change of discharge curves with C-rates (0.1, 1, 2, 4 and 10C) after CC–CV charging at 0.2 C to 4.2 V at room temperature for PAN based pouch type full cell.

*3.2.2. Cycle properties*

To observe capacity deterioration behavior of each battery with repeated charge and discharge at 25 °C and 45 °C, the electrochemical durability at the 1 C/1 C charge/discharge rate was examined. In terms of the battery life, at room temperature (25 °C), both separators showed very similar cycle life without any capacity fading. On the other hand, the newly developed PAN-separator-based battery showed comparatively better durability at high temperature (45 °C), as shown in the Fig. 3.

To observe the morphological change between the two separators after 100 cycles, each battery was fully discharged at the end of the 100th cycle. Then, each pouch cell was disassembled, and SEM analysis was performed to see how the surface morphology of each separator had been changed (due to oxidation reaction, etc.). As shown in Fig. 4, either separator's morphology was hardly changed at room temperature. At high temperature, the PE based cell, however, might be observed to be a little gradual deterioration in battery life due to the blocking of air holes in separator. Although the PAN separator had a thin organic film on its surface, it could be observed that this type of film would be not enough to block the separator's air holes. Therefore, it is confirmed that the cyclic degradation was meaningfully attributed to separator pore clogging

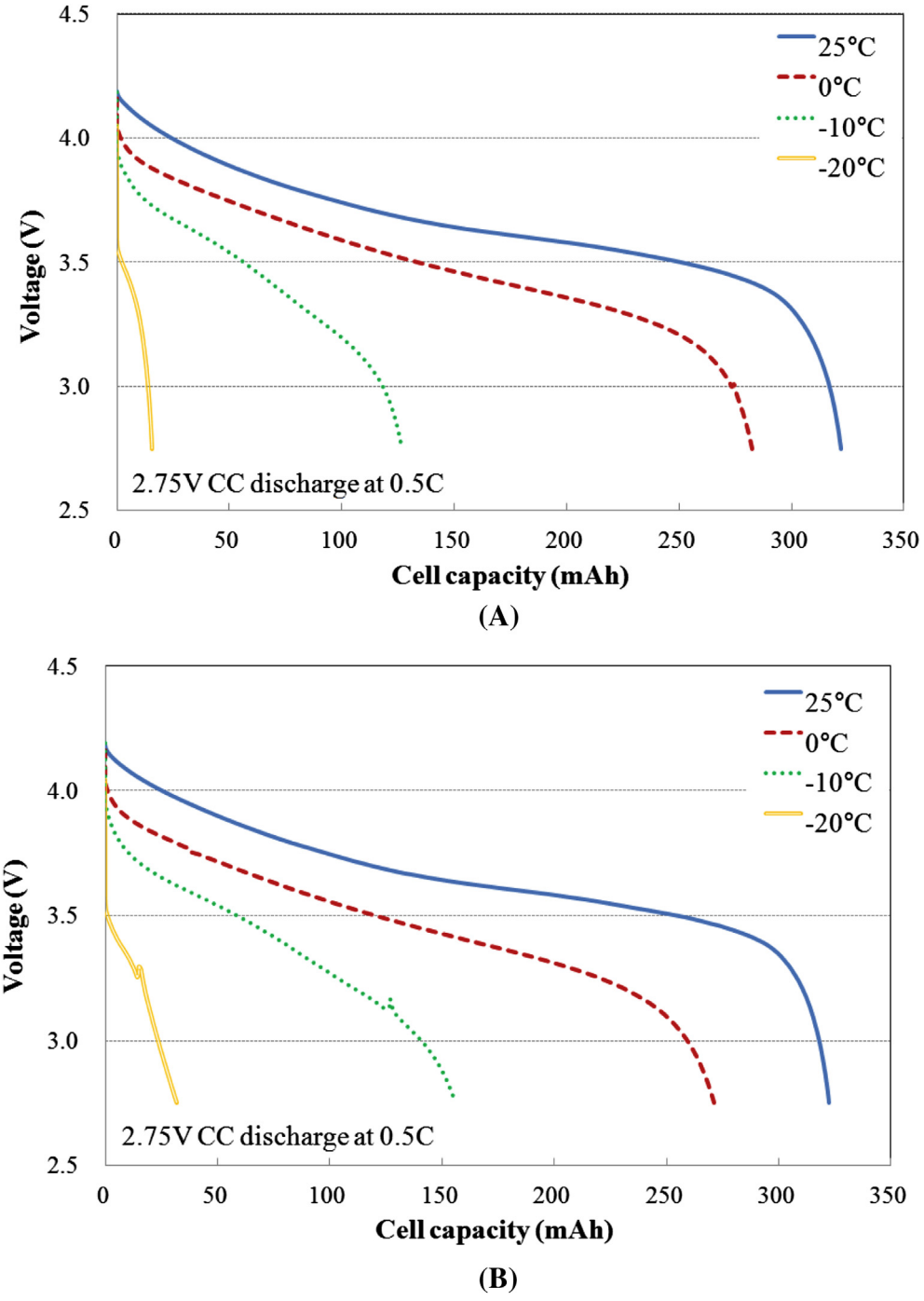


**Fig. 7.** Comparison of discharge curves with different temperatures (25 °C, 0 °C, −10 °C, and −20 °C) for pouch type full cell with (A) PE and (B) PAN separators.

**Table 4**
Temperature dependence of discharge capacity for pouch type full cell with (A) PE and (B) PAN separators.

| Temperature | PE separator based cell | | PAN separator based cell | |
|---|---|---|---|---|
| | Capacity (mAh) | $C_T/C_{25\,°C}$ (%) | Capacity (mAh) | $C_T/C_{25\,°C}$ (%) |
| 25 °C | 321 | 100 | 322 | 100 |
| −0 °C | 282 | 87.9 | 271 | 84.1 |
| −10 °C | 126 | 39.4 | 156 | 48.4 |
| −20 °C | 16 | 4.9 | 32 | 9.9 |

induced by electrochemical oxidation in interface between electrode and separator during cyclic electrochemical operation.

Fig. 5 shows comparison of each separator's Gurley value with as-prepared one after 100th cycle at room temperature (25 °C) and high temperature (45 °C). Less Gurley value implies that it takes less for a corresponding separator to penetrate through a certain volume Compared to the PE separator, the PAN separator showed less Gurley value, which could be also expected by physical parameters of each separator. That means the air-penetration path is reduced by a well-formed air hole structure (Table 3).

### 3.2.3. Rate capabilities & low-temperature discharge-ability

The high-rate and low-temperature discharge properties for pouch stack cells with one of the separators were evaluated. As shown in Figs. 6 and 7, the cell applying PAN based separator with higher air porosity showed relatively better high-rate properties and low temperature discharge-abilities. Temperature dependence of discharge capacity for pouch type full cell with PE and PAN separators is summarized in Table 4.

In general, at extremely high C-rate (i.e. 10 C, etc.), concentration polarization associated with the ion conductivity inside an electrolyte dominates over an activation polarization that is triggered by the interface resistance between the active material and the electrolyte. The difference in discharge capacity between batteries applying two kinds of separators seems to be getting noticeable at 10 C rate as shown in Fig. 6. It indicates the concentration polarization of batteries studied in this paper depends on separator's properties considering the rate capability of higher C-rate. Because the concentration polarization is closely related to ionic conductivity determined by a separator's morphologies, the AC impedance of battery was measured to determine the ionic conductivity in battery associated with a separator's air hole size. The ionic conductivity ($\sigma$) of battery can be derived from eq (1).

$$\sigma = L/R_b \cdot S \quad (1)$$

Where $L$ and $S$ are thickness and area of the separator, respectively, and $R_b$ is the bulk resistance obtained from the AC impedance test.

The bulk resistance of battery is determined by intercept point on real impedance between circle and $x$-axis at high frequency region in AC impedance spectra. The PAN separator showed higher ionic conductivity values that were derived from the real impedance values at high-frequency (100 kHz) than that of conventional separator based battery, as shown in the Fig. 8. It is, therefore, confirmed that the battery applying PAN based non-woven separator shows better high-rate and low-temperature performances due to higher ionic conductivity. In addition, based on the temperature-dependent impedance changes, the change of charge transfer resistance has a close relationship with temperature rather than separator morphologies. In particular, the changes in such values relating to the bulk resistance components measured at high frequency were more noticeable in case of battery with conventional separator.

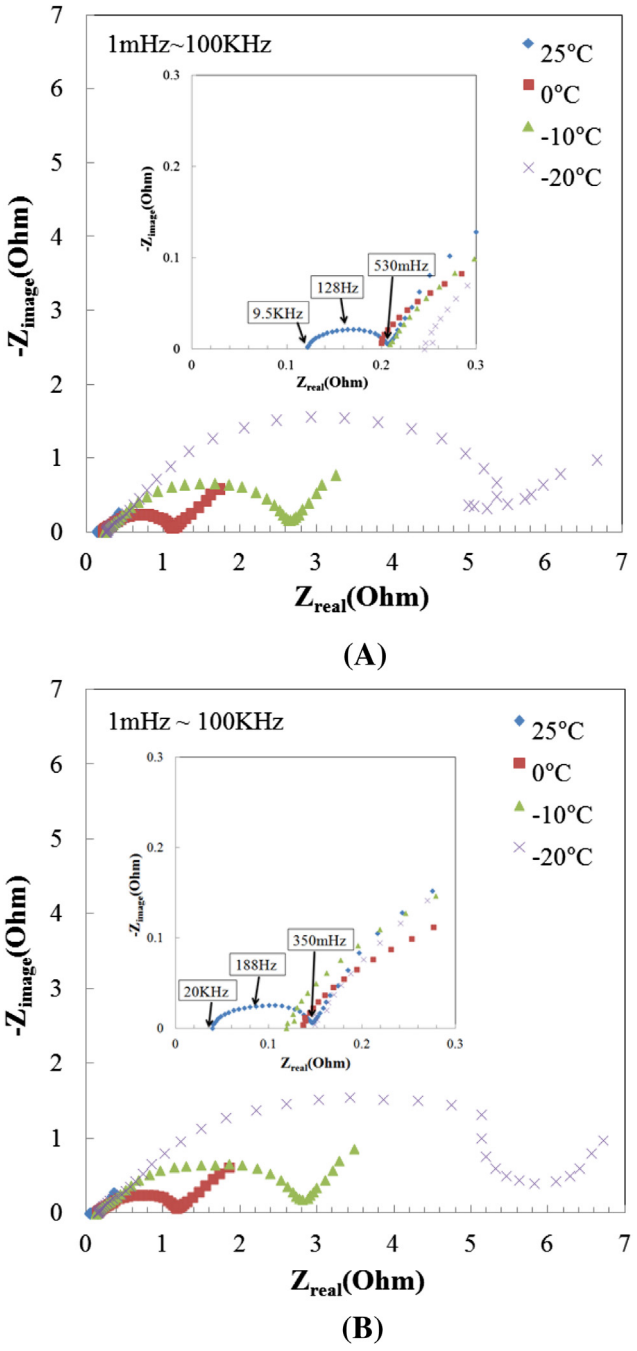


**Fig. 8.** Comparison of Nyquist plots with different temperatures (25 °C, 0 °C, −10 °C, and −20 °C) for pouch type full cell with (A) PE and (B) PAN separators.

Based on the AC impedance test results, therefore, the PAN separator's superior performance at high-rate and low-temperature conditions was mainly due to the size and distribution of its air holes.

## 3.3. Electrochemical stability

### 3.3.1. Electrochemical window stability (linear sweep voltammetry study)

In order to see how the PAN separator electrochemically reacts at high-voltage conditions (i.e. electrochemical oxidation condition), the related tests were implemented from two perspectives.

First, in order to observe the oxidation reaction and side reaction at certain high-voltage conditions, a cell with SS (Working electrode: Stainless steel blocking electrode)/separator-electrolyte (with $LiPF_6$, w/o $LiPF_6$)/Li (Reference electrode, counter electrode) was made for the LSV (Linear Sweep Voltammetry) test. As shown in the Fig. 9(A), there was almost no change in the onset voltage, which indicates the sudden occurrence of an oxidation reaction. Then, an LSV test that excluded $LiPF_6$ to remove any oxidation reaction current, which might be triggered by anion in dissociated salt, was conducted. As shown in Fig. 9(B), the very little parasitic current was generated for both separators even at high voltages up to 6 V, implying that there was no additional oxidation reaction triggered by the PAN separator.

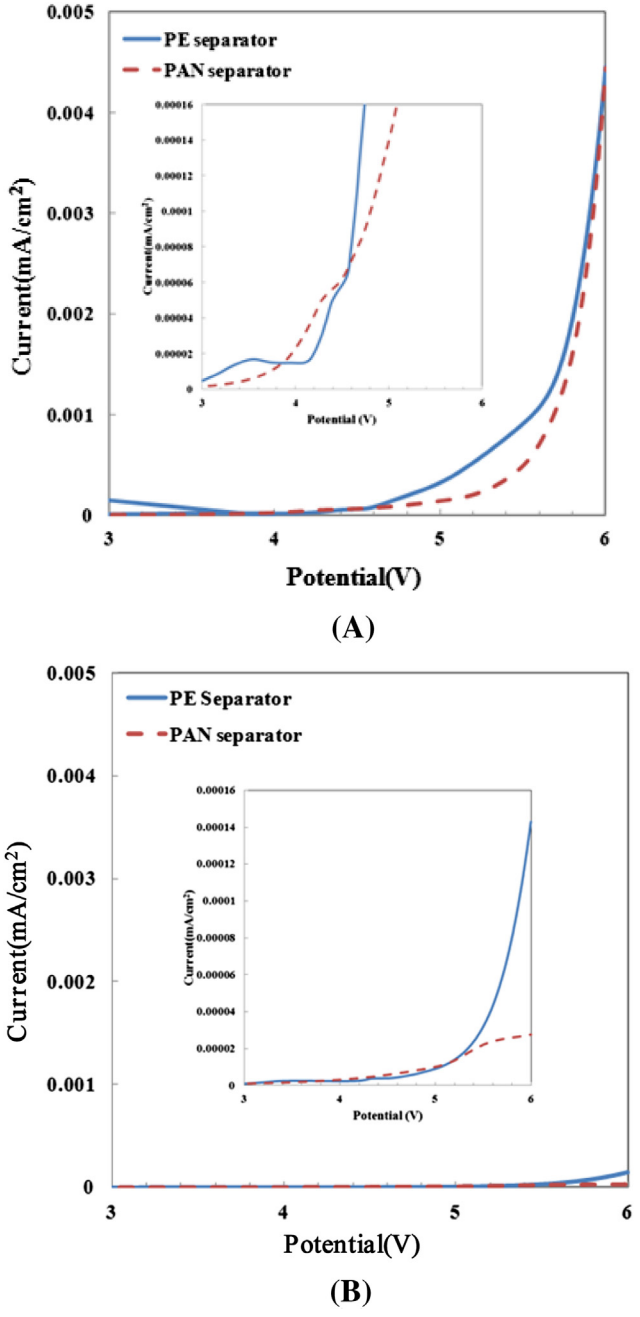


**Fig. 9.** Linear sweep voltammograms of each cell with SS/separator/Li pole at a scan rate 20 mV $s^{-1}$ applying EC:EMC = 1:2 (v/v) + VC 2 wt. % (A) with $LiPF_6$, and (B) without $LiPF_6$.

*3.3.2. Metal ion transfer*

A full cell for each separator was made with graphite/LNCMO and tested for trickling charging, which is a way of charging a battery at constant voltage (i.e. 4.3 V and 4.5 V) until the current reaches zero. In addition, SEM/EDS analysis was conducted to check for any metal dissolution on a fully-charged anode's surface or any metal dissolution on a corresponding cathode's surface. This test is used to prove that a PAN separator's air hole size can be regarded as a positive dynamical property like high-rate and low-temperature properties, but is closely related to the movement of undesired metal ions triggered by the shuttle mechanism.

As shown in the Figs. 10 and 11, after continuous charging at 4.2 V for hours, the PE based cell had no metal complex deposition on the interface between anode and separator, while the PAN based one had a trace of metal complex deposition, especially for such metals as Mn, Co and Ni. A similar phenomenon occurred when the battery life tests were repeated at room temperature and high temperature. Metal ion elution phenomenon triggered by the oxidation reaction between a fully-charged anode's surface and the electrolyte surface cannot be avoided, and this phenomenon becomes more apparent at high temperature and high-voltage conditions. Therefore, the PAN separator normally goes through a more influential metal ion transition phenomenon, and this kind of phenomenon becomes more serious at certain conditions (i.e. high temperature, repeated battery life evaluation, abnormal charging, etc.).

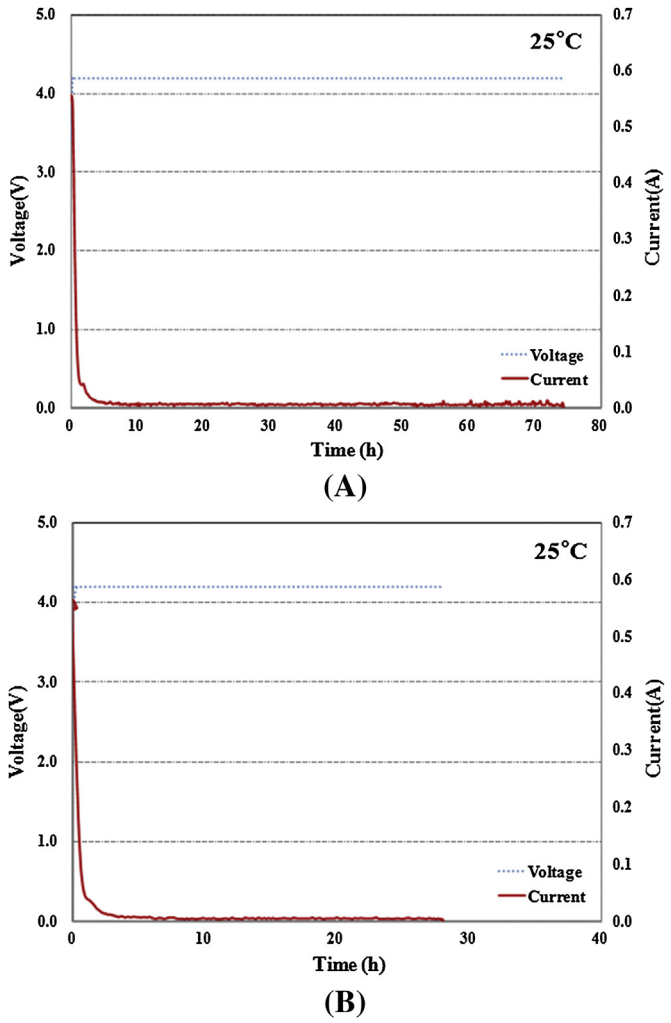


**Fig. 10.** Current profiles during continuous charging at 4.2 V to zero current for pouch type full cell with (A) PE and (B) PAN separators.

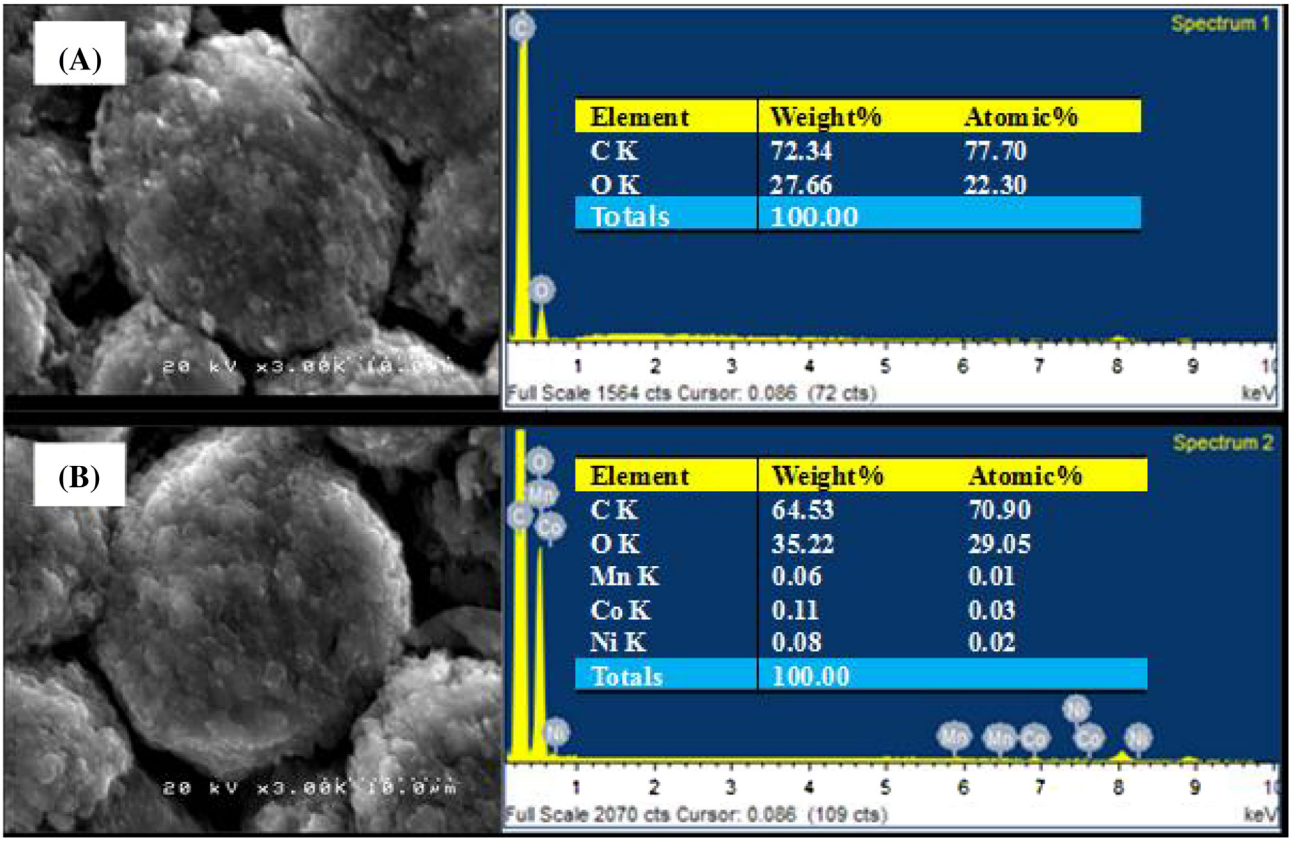


**Fig. 11.** Energy Dispersive Spectroscopy (EDS) analysis on anode surface after continuous charging at 4.2 V to zero current for pouch type full cell with (A) PE and (B) PAN separators.

### 3.4. Thermal stability

#### 3.4.1. Thermal contraction

In order to evaluate certain heat-resistant properties of separators developed in this study, test conditions similar to the 150 °C hot-box test (a standard test to evaluate the physical conditions of a jelly roll inside a real battery and its safety) were established. Each separator was positioned between slide glasses and subjected to certain tensile shear stress. Then, the temperature was raised up to 150 °C and 180 °C at 5 °C per minute, and both separators were kept

| | PE Separator | PAN Separator |
|---|---|---|
| As-prepared |  |  |
| | Size : 5cm x 2.5cm<br>Thermal shrinkage : 0% | Size : 5cm x 2.5cm<br>Thermal shrinkage : 0% |
| 150°C for 12h |  |  |
| | Size : 4.5cm x 2.1cm<br>Thermal shrinkage : 24.4% | Size : 5cm x 2.5cm<br>Thermal shrinkage : 0% |
| 180°C for 12h |  |  |
| | Size : 4cm x 1.8cm<br>Thermal shrinkage : 42.4% | Size : 5cm x 2.4cm<br>Thermal shrinkage : 4% |

**Fig. 12.** Comparison of thermal contraction behavior for each separator after 12 h at 150 °C, and 180 °C.

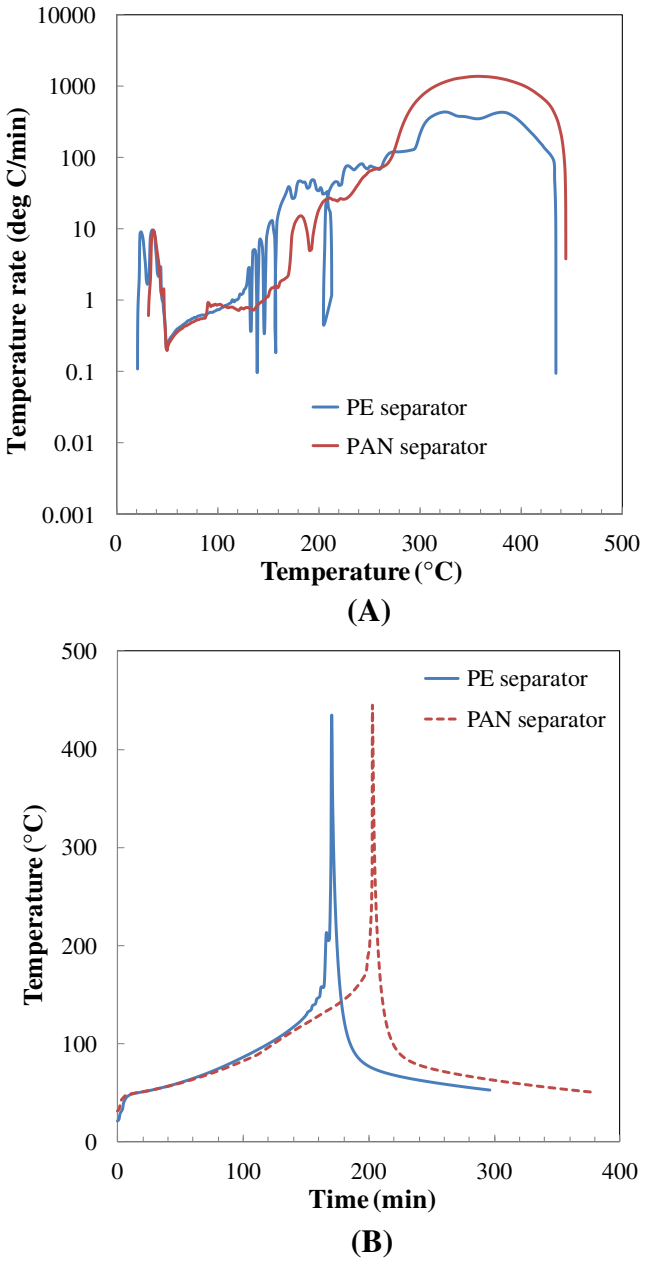


**Fig. 13.** Comparison of (A) exothermic rate and (b) thermal run-away behavior for pouch type full cell during accelerated rate calorimetric test.

for 12 h at each temperature in order to compare their contraction percentages. As shown in the Fig. 12, the PAN separator showed a contraction percentage close to 0% at 150 °C, while the PE separator showed a contraction percentage greater than 10% in both width and length. Moreover, at 180 °C, the PAN separator showed a contraction percentage equal to only 4%, while the PE separator showed a contraction percentage greater than 25%.

### 3.4.2. ARC behavior

In order to check the actual effects of thermal contraction behavior on a pouch full cell, ARC (Accelerated Rate Calorimetry) tests were performed. This test is designated to check the relative heat safety of battery. The ARC behavior of battery is mainly characterized by onset temperature for thermal runaway and self-exothermic heating rate at corresponding temperature. These key parameters on thermal safety of battery can be defined from temperature behavior with heating time. As shown in Fig. 13(A), regarding runaway temperature, the thermal runaway phenomenon of PAN based battery occurs at higher onset temperature (159 °C) than that of PE based battery (141 °C). In addition, the PAN based battery has lower self-exothermic reaction rate (i.e. PAN (0.78 °C $min^{-1}$) < PE (2.46 °C $min^{-1}$)) at 130 °C, thereby showing retardation effects on temperature and time until a thermal run-away of battery actually occurs (Fig. 13(B)). Therefore, based on the PAN separator's thermal contraction properties, it can be concluded that its thermal stability is much better than that of PE separator.

## 4. Conclusion

Cell performance, electrochemical stability, and thermal stability properties for both PE and PAN separators were extensively compared and analyzed. The overall evaluation result indicates that the cell applying PAN based non-woven separator showed superior performance over the PE separator's one. The better performances of PAN based cell was confirmed to be mainly attributed to higher ionic conductivity and lower thermal shrinkage properties of PAN based non-woven separator compared with conventional PE separator. However, in the continuous charging test, the PE separator didn't allow any transfer of metal ion, which was dissolved by oxidation reaction on the cathode surface, across air holes in separator, while the cell applying PAN separator had metal complex deposition on the anode surface, especially for such metals as Mn, Co and Ni. Going forward with this study, it is necessary to develop a composite separator that can prevent any metal transfer followed by deposition phenomenon while maintaining the PAN separator's positive performance, based on higher ionic conductivity.

## Acknowledgment

This work was supported by the Korea Evaluation Institute of Industrial Technology funded by the Ministry of Knowledge Economy (MKE-2012-10040033) and the National Research Foundation of Korea Grant funded by the Korean Government (MEST) (NRF-2011-C1AAA001-0030538).

## References

[1] M. Armand, J.M. Tarascon, Nature 451 (2008) 652.
[2] D. Linden, T.B. Reddy, Handbook of Batteries, third ed., McGraw-Hill, 2002.
[3] F. Croce, G.B. Appetecchi, L. Persi, B. Scrosati, Nature 394 (1998) 456.
[4] G. Venugopal, J. Moore, J. Howard, S. Pendalwar, Journal of Power Sources 77 (1999) 34.
[5] B.L. Luan, G. Campbell, M. Gauthier, X.Y. Liu, I. Davidson, J. Nagata, M. Lepinay, F. Bernier, S. Argue, ECS Transactions 25 (2010) 59.
[6] R.J. Brodd, H.M. Friend, J.C. Nardi, Lithium Ion Battery Technology, ITE-JEC Press, 1995.
[7] U. von Sacken, E. Nodwell, A. Sundher, J.R. Dahn, Solid State Ionics 69 (1994) 284.
[8] S. Tobishima, J.I. Yamaki, Journal of Power Sources 81 (1999) 882.
[9] J.I. Yamaki, in: M. Wakihara, O. Yamamoto (Eds.), Lithium Ion Batteries, 83, Kodansha and Wiley-VCH, Tokyo (Japan), 1998.
[10] J. Cho, Y.J. Kim, T.J. Kim, B. Park, Chemistry of Materials 13 (2001) 18.
[11] H.J. Kweon, S.J. Kim, D.G. Park, J. Power Sources 88 (2000) 255.
[12] R.A. Leising, M.J. Palazzo, E.S. Takeuchi, K.J. Takeuchi, Journal of the Electrochemical Society 148 (2001) A838.
[13] A.N. Dey, Journal of the Electrochemical Society 118 (1971) 1547.
[14] A.M. Christie, S.J. Lilley, E. Staunton, Y.G. Andreev, P.G. Bruce, Nature 433 (2005) 50.
[15] A. Manuel Stephan, European Polymer Journal 42 (2006) 21.
[16] F.G.B. Ooms, E.M. Kelder, J. Schoonman, N. Gerrits, J. Smedinga, G. Callis, Journal of Power Sources 97–98 (2001) 598.
[17] H.S. Jeong, J.H. Kim, S.Y. Lee, Journal of Materials Chemistry 20 (2010) 9180.
[18] T.H. Cho, M. Tanaka, H. Onishi, Y. Kondo, T. Nakamura, H. Yamazaki, S. Tanase, T. Sakai, Journal of Power Sources 181 (2008) 155.

[19] Y. Lee Min, J.W. Kim, N.S. Choi, J. Lee An, W.H. Seol, J.K. Park, Journal of Power Sources 139 (2005) 235.
[20] M. Tanaka, T.H. Cho, T. Nakamura, T. Tarao, M. Kawabe, T. Sakai, Electrochemistry 78 (2010) 982.
[21] Y. Liang, L. Ji, B. Guo, Z. Lin, Y. Yao, Y. Li, M. Alcoutlabi, Y. Qiu, X. Zhang, Journal of Power Sources 196 (2011) 436.
[22] P. Kritzer, J.A. Cook, Journal of the Electrochemical Society 154 (2007) A481.
[23] T.H. Cho, T. Sakai, S. Tanase, K. Kimura, Y. Kondo, T. Tarao, M. Tanaka, Electrochemical and Solid-State Letters 10 (7) (2007) A159.
[24] T.H. Cho, M. Tanaka, H. Ohnishi, Y. Kondo, M. Yoshikazu, T. Nakamura, T. Sakai, Journal of Power Sources 195 (13) (2010) 4272.
[25] E.P. Roth, D.H. Doughty, Journal of Power Sources 128 (2004) 308–318.
[26] I. Uchida, H. Ishikawa, M. Mohamedi, M. Umeda, Journal of Power Sources 821 (2003) 119–121.
[27] P.X. Ma, R. Zhang, Journal of Biomedical Materials Research 46 (1999) 60.
[28] D.H. Reneker, I. Chun, Nanotechnology 7 (1996) 216.
[29] K.J. Kim, J.H. Kim, M.S. Park, H.K. Kwon, H.S. Kim, Y.J. Kim, Journal of Power Sources 128 (2012) 298–302.